Research and Reviews in Materials Science and Chemistry
Vol. 3, Issue 2, 2014, Pages 97-114
ISSN 2319-6920
Published Online on June 2, 2014

http://jyotiacademicpress.net

SYNTHESIS OF ALUMINUM SILICATE NANOFLAKES IN PRESENCE OF L-ARGININE AMINO ACID BY SOL-GEL PROCESS

H. A. MONREAL[1,2], A. MARTÍNEZ VILLAFAÑE[2], C. A. MARTÍNEZ[3], P. E. CASILLAS[3], J. MORA[4], R. PÁJARO[1] and J. G. CHACON NAVA[2]

[1]Facultad de Odontología
U.A.CH. Ciudad Universitaria Campus I Chihuahua
México
e-mail: hmonreal@uach.mx

[2]Centro de Investigación en Materiales Avanzados S.C.
(CIMAV) and Laboratorio Nacional de Nanotecnologia
Av. Miguel de Cervantes 120
Complejo Industrial Chihuahua
CP 31109 Chihuahua
México

[3]Instituto de Ingeniería y Tecnología
U.A.C.J. Avenida del Charro # 610 Norte
Cd. Juárez, Chihuahua
México

[4]Facultad de Ingeniería
Universidad Autónoma de Chihuahua
Nuevo Campus Universitario
S/N, C.P. 31125
Chihuahua, Chih.
México

Keywords and phrases: nanoflakes, sol-gel method, L-arginine amino acid, aluminum-silicate, scanning tunneling microscopy.

Communicated by Ana Rosa Silva.

Received February 24, 2013; Revised May 5, 2014

Abstract

In this work, we report the synthesis of aluminum silicate nanoflakes in presence of linear L-arginine amino acid through the sol-gel method. A solution containing aluminum silicate and hydrochloric acid was prepared and after, L-arginine amino acid was added as template up to gel formation. The gel was dried at 200ºC and the powder was characterized by means of X-ray diffraction, scanning tunneling microscopy (STM), electron microscopy (SEM), energy dispersive spectroscopy (EDS), thermogravimetric analysis (TGA), differential thermal analysis (DTA), and IR spectroscopy. The nanostructures' diameter obtained ranged from 5nm to 50nm with a thickness of about 6nm. The nanoflakes surface area was about $230.19(m^2/g)$. The results show the effect in vitro of L-arginine in the nanoflakes synthesis. These materials can be useful for structured materials, dental materials, and molecular electronics.

1. Introduction

The development of new materials at molecular levels has increased due to generations of materials, designs, synthesis, and devices manufacturing at molecular scale, also taking into account the supramolecular chemistry of different metals in biological systems [1]. The principles of the supramolecular complexes micro-manufacturing in biological macromolecules can be understood by means of their electrostatic and topographic properties [2]. The functional proteins role in the modification of dental enamel structure has been developed in other studies [3]. Several systems have been studied as models for determining the glass-ionomer with amino acids interaction [4] or for the study of aluminum-silicate with chlorohexidine antibacterial properties [5]. The basic principles for micro-manufacturing can be understood by means of supramolecular chemistry, which is present in nature. The supramolecular chemistry key components are the chemical complementary and the electrostatic interactions structural compatibility [6]. Recent advances in amino acid chemistry have resulted in the development of new materials [7]. The addition of cations such as poly-L-lysine by physiological means, leads to the spontaneous assembly of these oligopeptides to form microscopic and macroscopic structures that

can be built into different geometric forms [8]. One of the self-assembly systems proposed as a study model is the one formed by the poly-L-lysine peptide, where the positive charges interact with the glutamate negative ones, forming folded molecular structures [1]. Also, another self-assembly model system consists of a cetyltrimethylammonium solution (CTMA) to which DNA molecules are added, thus forming laminar structures where the negative charges of the DNA interact with the CTMA positive ones [9]. In other studies, human serum albumin based nanotubes have been synthesized with-L-arginine [10]. In addition, the work by Cao et al. [11], reported the use of L-arginine to form films with gold nanoparticles to determine case in by an electrochemical immuno sensor. In this context, we are reporting the synthesis of $AlSiO_2$ nanoflakes in presence of L-arginine.

2. Experimental Details

The experimental procedure for the synthesis of aluminum silicate nanostructures in the presence of L-arginine amino acid ($C_6H_{14}N_4O_2$ BioChemika Ultra > 95% NT), was designed through the sol-gel method in three steps [12]. In the first step, a solution was prepared containing 30mg of aluminum silicate and 70µl of hydrochloric acid (42% w/v). In the second step, 5ml of hydrochloric acid were mixed with 10ml of bi-distilled water (50% v/v). Last, this solution was slowly added to the first one, and stirred in a magnetic stirrer for 24h until the aluminum-silicate sol was formed. In the three steps, the samples were aged at room temperature for 10 days, and then a template was added (375mg of L-arginine). Afterwards, the solution containing the template was dried for 7 days, thus forming the gel. Finally, the gel was heated at 200ºC. To optimize the nanoflakes formation, several experiments were conducted by modifying the solutions concentration used.

The STM images were obtained by using a Nanosurf Easy Scan II instrument, which is equipped with Pt/Ir tips (BT00400). The images were processed by using an easy scan image software version 1-6-0-0. All samples were prepared by deposition of an aliquot (5μl, 5mM Phosphate Buffer Saline solution pH 7.2) on a silicon wafer. After this, the wafers were calcined at 100°C and stored in 10mM isopropanol until their use. In addition, the nanoflakes were characterized by means of scanning electron microscopy (SEM) and energy dispersive spectroscopy (EDS). For the DTA-TGA analysis, the samples were heated at a heating rate of 10°C/min in air. Diffraction patterns were obtained in a Phillips X-ray diffractometer X'PERT, and the BET surface area was determined by nitrogen adsorption (Quantachromeautosorb). In order to obtain the stress-strain curve, PASCO AP-8214 equipment was used. Specimens were prepared in cubes of $14\text{mm} \times 14\text{mm}$, being similar to the samples reported by Nikhil & William [13] and Lessard [14]. In a solid matrix, 1g of aluminum silicate/L-arginine in 20μl of maleic acid ($C_4H_4O_4$ 1M) was added. Since maleic acid absorbs less water, this might improve the composites dimensional stability. Afterwards, the samples were polished with a fine paste of aluminum oxide, then washed with 50ml in de-ionized water, and dried at 37°C. The infrared spectra samples (wave number range of 1200cm^{-1} to 4000cm^{-1}) were obtained by using a Perkin-Elmer infrared spectrophotometer. Morphological features were taken by using a scanning electron microscope (SEM) JEOL JSM-5800 LV/EDS.

3. Results and Discussion

3.1. Characterization by STM and SEM

Scanning tunneling microscope (STM) is a tool that has been used for the characterization of materials surface at a structural level. The results of STM measurements gave evidence that nanoflakes were formed in solution. Figure 1(a) shows an STM image of aluminum-silicate without

L-arginine amino acid. Images 1(b) and 1(c) correspond to aluminum-silicate plus L-arginine amino acid. Here, it is possible to observe the nanostructures formation. These nanostructures are mostly nanoflakes with a thickness of about 6nm and a diameter in a range of 5nm up to 50nm. The centre-to-centre distance between atoms was 10nm-105nm. This observation is also supported by the root mean square (RMS) roughness values. This value corresponds to arms roughness of 28.5nm. Figure 1(d) shows another view of the nanoflakes formed.

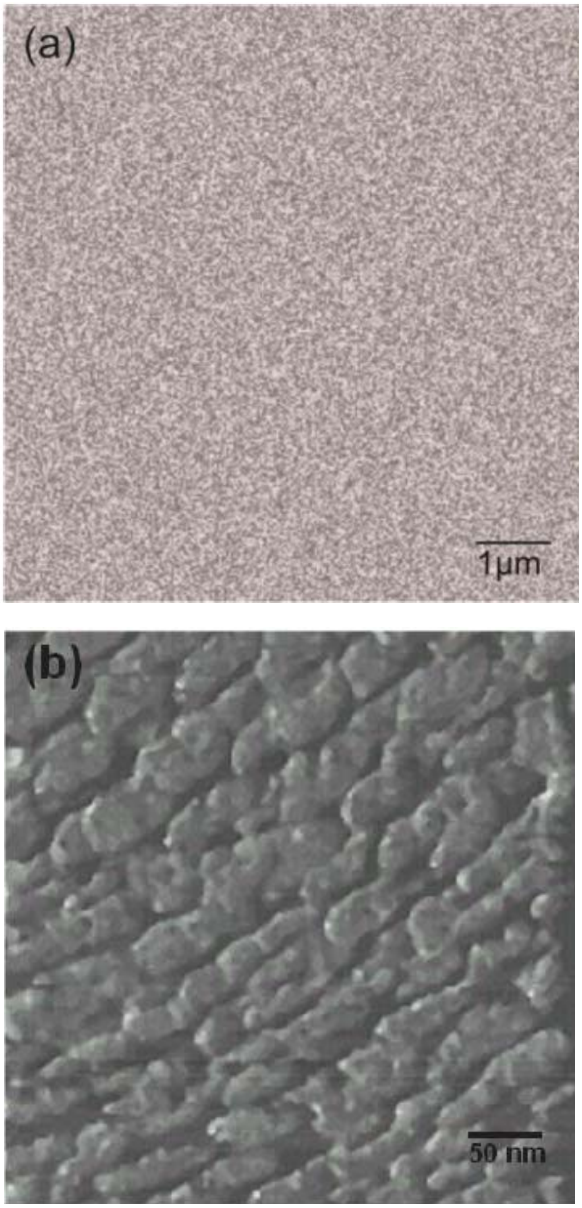
(a)
1μm
(b)
50 nm

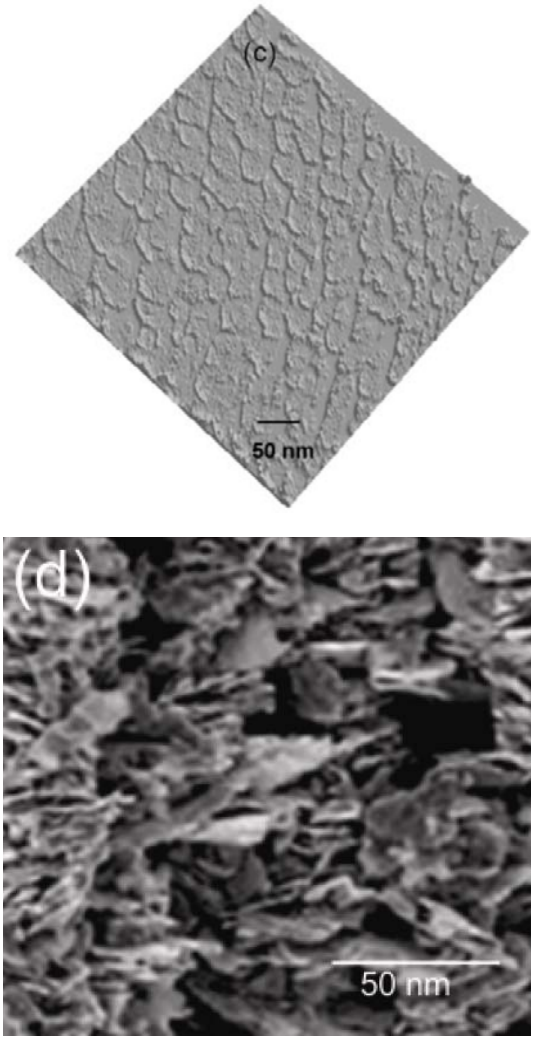

Figure 1. STM images of aluminum silicate/L-arginine composite, (a) aluminum silicate in absence of L-arginine; (b) aluminum-silicate nanoflakes in presence of L-arginine; (c) 3-D projection of the aluminum-silicate nanoflakes; and (d) SEM morphologies of aluminum-silicate nanoflakes.

3.2. Energy dispersive spectroscopy

Figure 2 shows the chemical composition of the nanoflakes analysed by EDS. The result indicates the presence of O, Al, and Si as the main elements. This analysis is important because it confirms that the nanoflakes are effectively composed of Al and Si with no contamination indication.

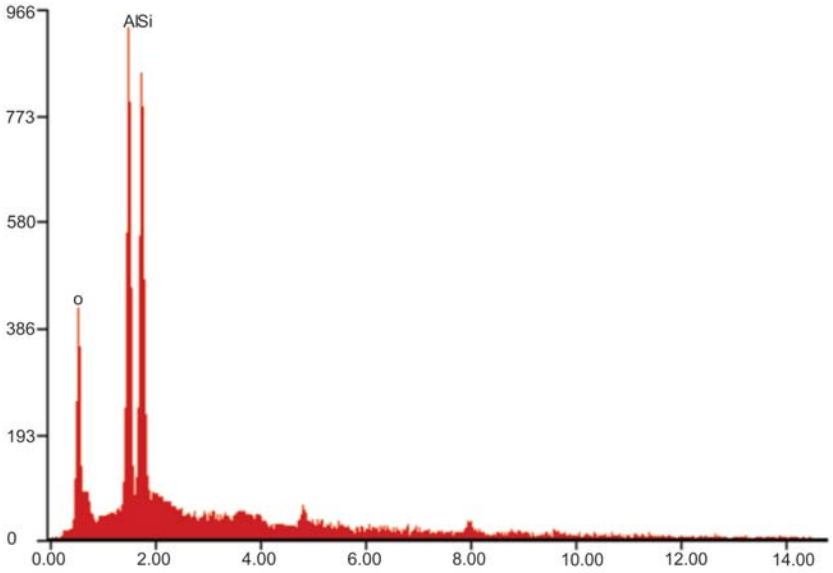

Figure 2. Typical EDS spectrum of the nanoflakes obtained.

3.3. Size distribution

Figure 3 shows the found nanoflakes' size distribution. The size distribution plot shows that most of the nanoflakes obtained in this work are in the range of about 5nm-50nm diameter (confirming the previous observations). Small nanoflakes sizes (4nm-10nm) have been reported using methods such as the microwave route [15]. Thus, the observed shape and size could be induced and controlled by the amino acid in the liquid phase. To some extent, the aluminum silicate addition prevents the nanoflakes growth in an orderly manner. In order to ensure that the

amino acid controls the nanoflakes morphology, several control experiments were carried out during the nanoflakes formation, as shown on Table 1.

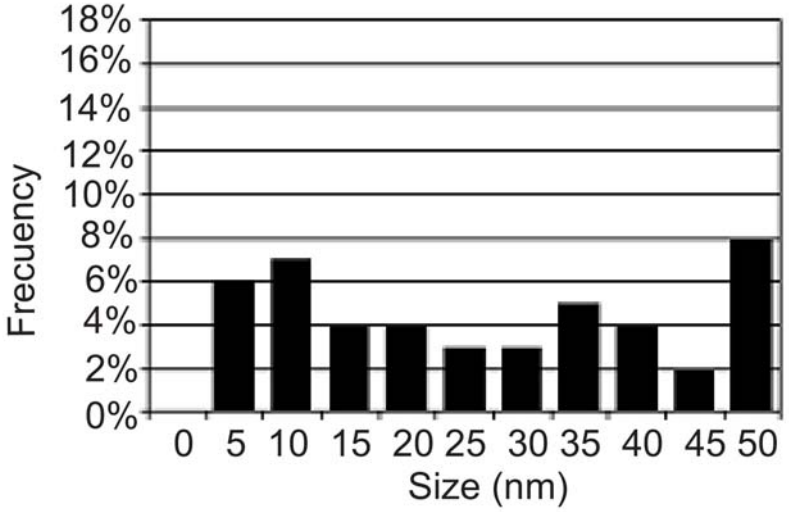

Figure 3. Size distribution of the nanoflakes.

Table 1. Experiments realized during the synthesis of nanoflakes

#	Step 1 (w/v)	Step 2 (v/v)	Step 3 L-arginine [mg]	Images SEM
1	10mg aluminum silicate + 70µl hydrochloric acid (14%)	1ml hydrochloric acid +10ml H_2O (10%)	23.4mg	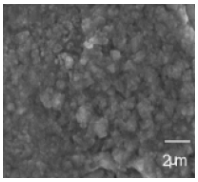
2	20mg aluminum silicate + 70µl hydrochloric acid (20%)	2ml hydrochloric acid +10ml H_2O (20%)	46.8mg	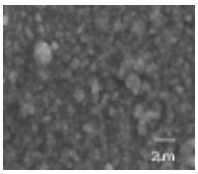
3	30mg aluminum silicate + 70µl hydrochloric acid (42%)	5ml hydrochloric acid +10ml H_2O (50%)	375mg	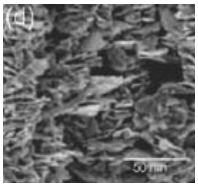
4	40mg aluminum silicate + 70µl hydrochloric acid (57%)	3ml hydrochloric acid +10ml H_2O (30%)	93.7mg	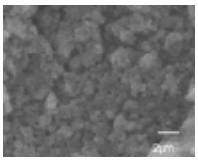
5	50mg aluminum silicate + 70µl hydrochloric acid (71%)	4ml hydrochloric acid +10ml H_2O (40%)	187.5mg	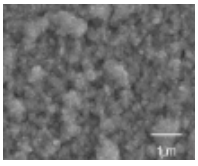
6	60mg aluminum silicate + 70µl hydrochloric acid (85%)	6ml hydrochloric acid +10ml H_2O (60%)	398.4mg	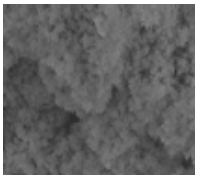
7	70mg aluminum silicate + 70µl hydrochloric acid (100%)	7ml hydrochloric acid +10ml H_2O (70%)	445.2mg	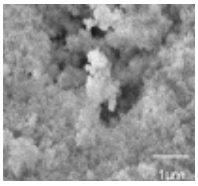

Table 1 (continued)

8	80mg aluminum silicate + 70µl hydrochloric acid (114%)	8ml hydrochloric acid +10ml H_2O (80%)	538.9mg	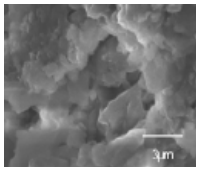
9	90mg aluminum silicate + 70µl hydrochloric acid (128%)	9ml hydrochloric acid +10ml H_2O (90%)	726.4mg	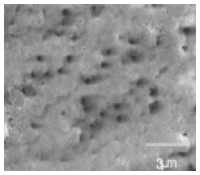
10	100mg aluminum silicate + 70µl hydrochloric acid (142%)	10ml hydrochloric acid +10ml H_2O (100%)	776.4mg	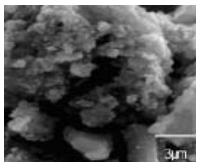
11	110mg aluminum silicate + 70µl hydrochloric acid (157%)	11ml hydrochloric acid +10ml H_2O (110%)	826.4mg	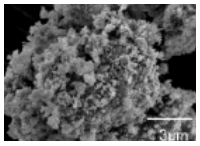

We studied the function of L-arginine in the aluminum-silicate nanostructures formation, and our hypothesis for the mechanism is that, the amino acid in a basic medium is ionized releasing a carboxyl group proton with loss of a water molecule; this way, the amino acid molecule retains the free anion. Furthermore, the hydroxyl group (OH^-) of the ionized water molecule can react with the Al^{+3} ions and form $Al(OH)_3$, Figure 4. There are many models proposed for the nanostructures' synthesis with amino acids, but none explains the self-assembly effect between inorganic and biological molecules. In other studies made with peptides, such as poly-L-lysine, where the silica synthesized structures disclosed diameters of about 30nm to 600nm, it has been reported that the diameter depends on the peptides concentration [16]. The surface area result is an important characteristic in the nanostructures synthesis, particularly when macromolecules like DNA and amino acids

are used between 200ºC-700ºC, even though other characteristics such as formation of more crystalline phases have not been extensively studied. The STM characterization reveals a dynamic process associated to the $AlSiO_2$ pairs of atoms and the L-arginine. We suggest that there is an electrostatic interaction between the $AlSiO_2$ atoms and the L-arginine amino acid. This could explain why atoms can reach the surface, remain attached and diffuse within the organic-inorganic complex. This may prevent the atoms separation, thereby retaining the nanoflakes' geometric structure.

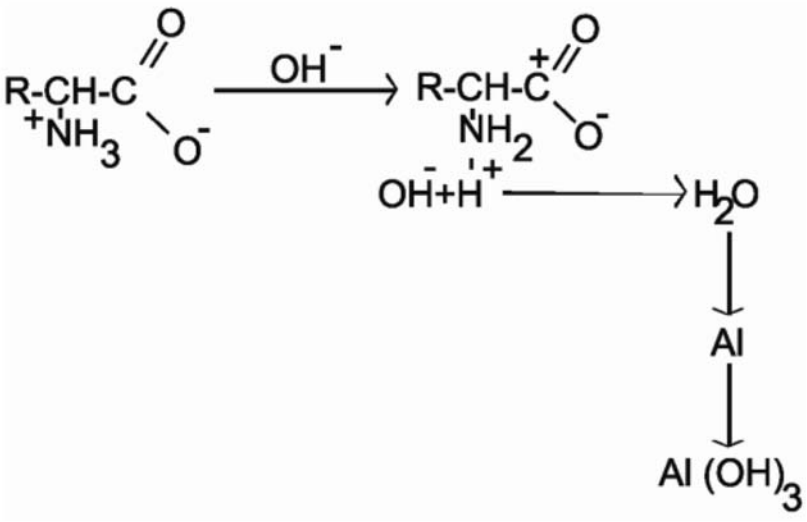

Figure 4. Scheme showing the mechanism of nanoflakes synthesis.

3.4. Thermal analysis

Figure 5 shows the compounds thermogravimetric measurements. In image 5(a), the weight loss was recorded at 100ºC, and it was accompanied by an endothermic peak at about 300ºC shown in image 5(b).

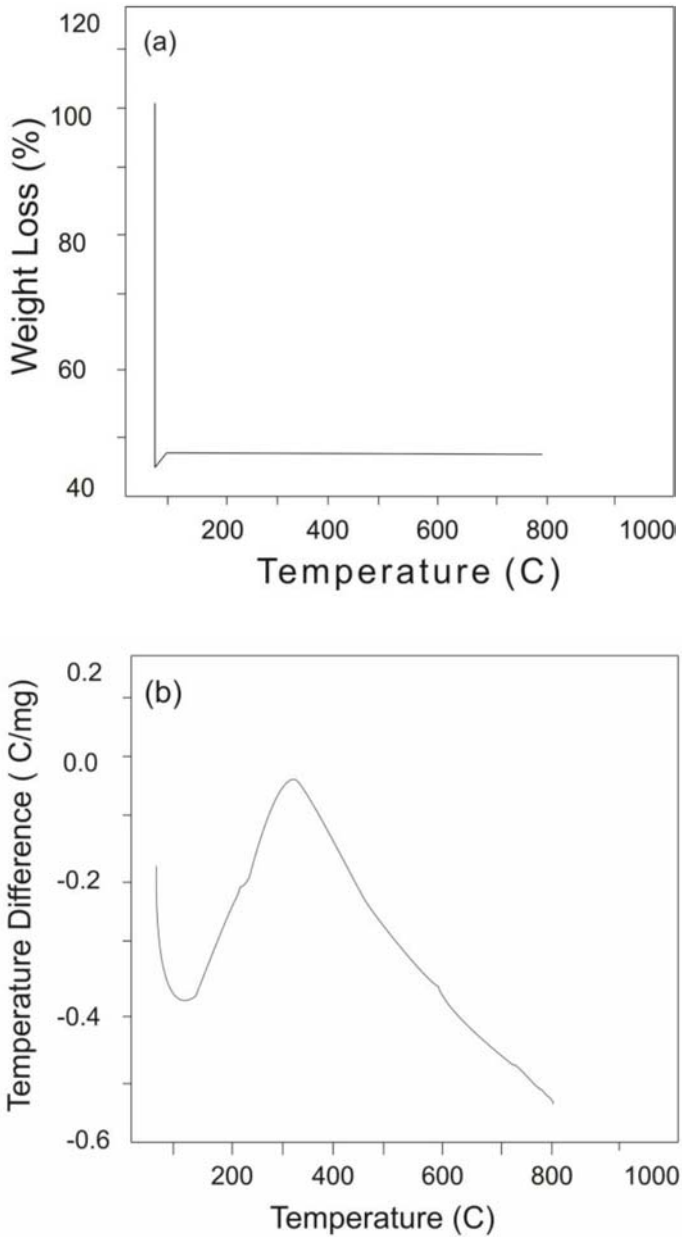

Figure 5. (a) TGA and (b) DTA analysis of aluminum-silicate in the presence of L-arginine.

3.5. X-ray diffraction and BET analysis

According to the XRD pattern showed in Figure 6, it was found that the obtained aluminum-silicate nanoflakes with L-arginine amino acid show the crystalline phase of aluminum-silicate at 200°C, which is characterized by several peaks with the 2θ diffraction angle in the range of 10°-15°. In this pattern, these peaks correspond to SiO_2, $Al(OH)_3$, and arginine, respectively, demonstrating the sample's crystalline nature. These results give evidence supporting the nanoflakes' formation mechanism proposed in Figure 4. Additionally, the BET nanoflakes surface area was about $230.19(m^2/g)$.

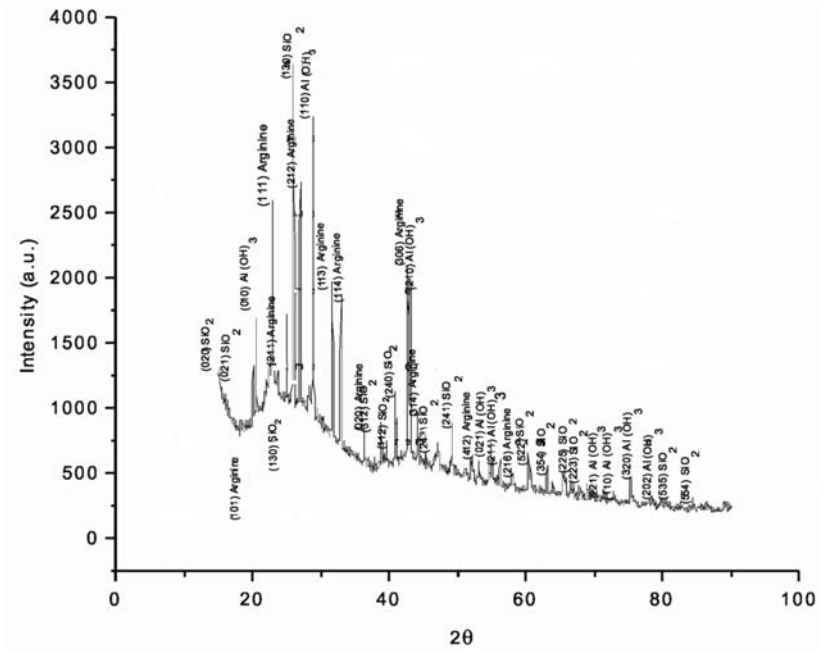

Figure 6. XRD pattern of aluminum-silicate nanoflakes in presence of L-arginine.

3.6. Stress-strain analysis

The stress-strain behaviour is shown in Figure 7. For the aluminum silicate/L-arginine compound, the results indicate a strain of 96% and a maximum stress of 90MPa, Figure 7(a). We believe that this compound disclosed high flexion due to the O_2 group interaction with the H from the L-arginine polymer chains. As seen on Figure 7(b), the previous mechanical trend is not observed for the aluminum silicate in absence of peptide. Thus, according to these results, the influence of the peptide on the mechanical behaviour becomes very important. In our case, Hooke's law is not observed because the stress is proportional to strain and the results do not follow a straight line in the curve. In any case, this would not be a negative situation for the nanoflakes production, since the behaviour of the stress-strain curves also depends on the nature of each material.

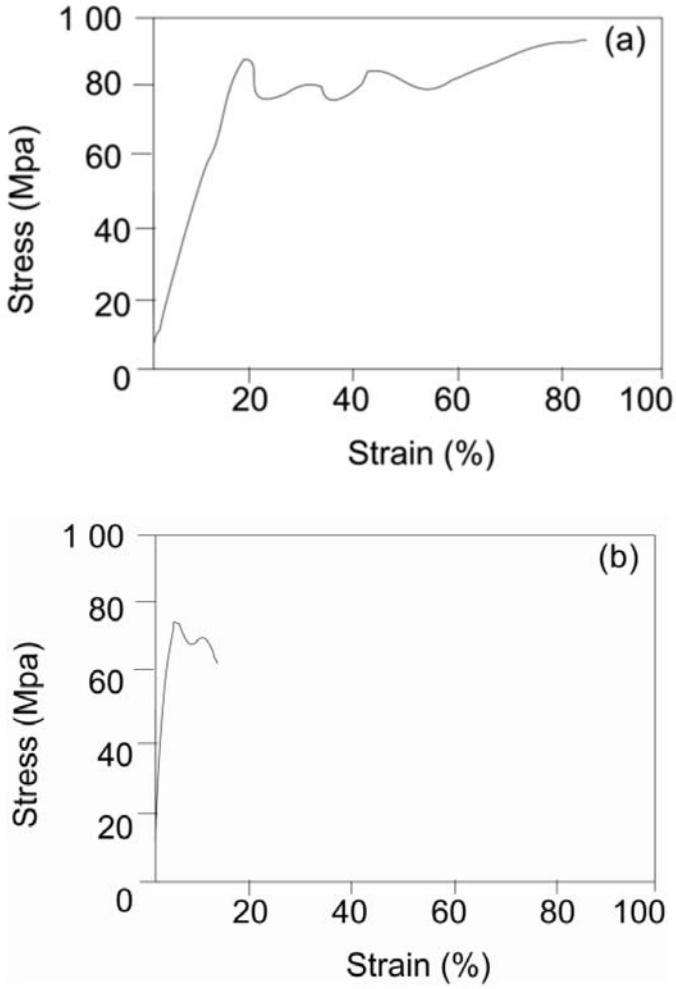

Figure 7. Stress-strain curve for (a) aluminum silicate/L-arginine; (b) aluminum silicate in absence of L-arginine.

3.7. IR spectrum

Figure 8 shows the absorption peaks of the IR spectrum revealing the ones corresponding to L-arginine. A band appears in the IR spectrum at $3500cm^{-1}$ due to NH stretching; another band appears at $1480cm^{-1}$, and next one at $1500cm^{-1}$, which corresponds to the NH_2 group bonding. To some extent, this indicates that arginine binds H and also to

the carboxyl groups leaving a partial negative charge and a partial positive charge, and those electrical charges can continue interacting with other ions in the medium.

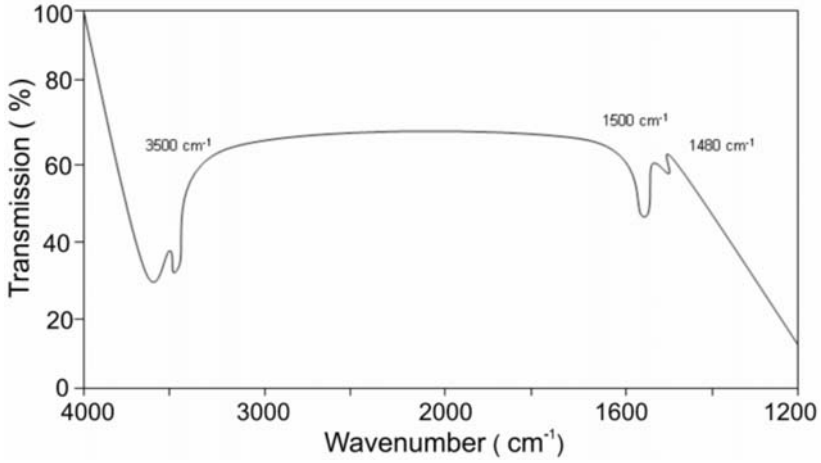

Figure 8. IR spectra of nanoflakes complex.

4. Conclusion

The use of L-arginine amino acid in this work demonstrates its capability to produce $AlSiO_2$ nanoflakes. Through the technique used, nanoflakes ranging from 5nm-50nm in diameter and 6nm in thickness can be produced and find potential uses in areas as material science and bio-nanomaterials. The L-arginine IR spectra measurement can also be used to study the structural vibrations phenomenon in the synthesis of hybrid materials to molecular scale. In this context, in order to synthesize the nanostructure, several events are required: (i) amino acid hydrolysis; (ii) linking of the amino acid chain during the polymerization by means of hydrogen bonds; (iii) addition of a metallic precursor to the amino acid; (iv) the nanoflakes formation; and (v) nanoflakes recovery after drying. With this method, it would be possible to study several aspects of the nanomaterial function in a biological complex. STM can be used to study the nanoflakes structure and the biological molecules adsorption into metallic precursors. Other interest studies being carried

on at present are (a) the amino acid functionality and the effect of its concentration on other materials synthesis, and (b) the effect of the amino acid in the metallic oxides polymerization at molecular level.

Acknowledgement

The authors would like to thank Enrique Torres and Wilber Antúnez for their technical assistance.

References

[1] D. Marini, W. Hwang, D. A. Laurenburger, S. Zhang and D. Kamm, Nano Lett. 2 (2002), 295-299.

[2] U. B. Sleytr, P. Messner, D. Pum and M. Sara, Angew. Chem. 111 (1999), 1098-1120.

[3] A. G. Fincham, J. Moradian, J. P. Oldak and J. Simmer, Struct. Biol. 126 (1999), 270-299.

[4] C. Beata and W. N. John, Dent. Mater. 22 (2006), 133-137.

[5] T. Yusuke, I. Satoshi, V. Andrea, S. E. Kaneshiro and R. T. Franklin, Dent. Mater. 22 (2006), 647-652.

[6] S. Zhang, Biotechnol. Adv. 20 (2002), 321-339.

[7] W. A. Petka, K. J. Harden, D. L. McGrath, P. Wirtz and D. A. Tirrell, Sci. 28 (1998), 389-392.

[8] Su X. Holmes, A. Delacalle, S. Rich and S. Zhang, Proc. Natl. Acad. Sci. USA, 97 (2000), 6728.

[9] W. Lili, Y. Jonichi and O. Naoya, Chem. Mater. 13 (2001), 1273-1281.

[10] Li. Moskovits and T. L. Haslett, Chem. Mater. 10 (1998), 1963-1967.

[11] Q. Cao, H. Zhao and Y. Yang, Bios. Bioel. 26 (2011), 3469-3474.

[12] M. Zhang, Y. Bando, K. Wada and K. Kurashima, J. Mater. Sci. Lett. 18 (1999), 1911-1913.

[13] G. Nikhil and R. William, Journal of Materials Processing Technology 198 (2008), 178-182.

[14] M. Lessard, ACI Materials Journal 90 (1993), 303-308.

[15] C. R. Patra, S. Patra, A. Gabashvili, Y. Mastai, Y. Koltypin, A. Gedanken, V. Palchik and M. A. Slifkin, J. Nanosci. Nanotechnol. 6 (2006), 845-851.

[16] N. Kröger, R. Deutzmann and M. Sumper, Science, Vol. 286, 1129-1132.

■